

THE NASA-UC ETA-EARTH PROGRAM:  
III. A SUPER-EARTH ORBITING HD 97658 AND A NEPTUNE-MASS PLANET ORBITING GL 785<sup>1</sup>

ANDREW W. HOWARD<sup>2,3</sup>, JOHN ASHER JOHNSON<sup>4</sup>, GEOFFREY W. MARCY<sup>2</sup>, DEBRA A. FISCHER<sup>5</sup>,  
JASON T. WRIGHT<sup>6</sup>, GREGORY W. HENRY<sup>7</sup>, HOWARD ISAACSON<sup>2</sup>,  
JEFF A. VALENTI<sup>8</sup>, JAY ANDERSON<sup>8</sup>, AND NIKOLAI E. PISKUNOV<sup>9</sup>

*Draft version June 10, 2018*

ABSTRACT

We report the discovery of planets orbiting two bright, nearby early K dwarf stars, HD 97658 and Gl 785. These planets were detected by Keplerian modelling of radial velocities measured with Keck-HIRES for the NASA-UC Eta-Earth Survey. HD 97658 b is a close-in super-Earth with minimum mass  $M \sin i = 8.2 \pm 1.2 M_{\oplus}$ , orbital period  $P = 9.494 \pm 0.005$  d, and an orbit that is consistent with circular. Gl 785 b is a Neptune-mass planet with  $M \sin i = 21.6 \pm 2.0 M_{\oplus}$ ,  $P = 74.39 \pm 0.12$  d, and orbital eccentricity  $e = 0.30 \pm 0.09$ . Photometric observations with the T12 0.8 m automatic photometric telescope at Fairborn Observatory show that HD 97658 is photometrically constant at the radial velocity period to 0.09 mmag, supporting the existence of the planet.

*Subject headings:* planetary systems — stars: individual (HD 97658, Gl 785) — techniques: radial velocity

1. INTRODUCTION

Radial velocity (RV) searches for extrasolar planets are discovering less massive planets by taking advantage of improved instrumental precision, higher observational cadence, and diagnostics to identify spurious signals. These discoveries include planets with minimum masses ( $M \sin i$ ) as low as  $1.9 M_{\oplus}$  (Mayor et al. 2009) and systems of multiple low-mass planets (Lovis et al. 2006; Fischer et al. 2008; Vogt et al. 2010). To date, 15 planets with  $M \sin i < 10 M_{\oplus}$  and 18 planets with  $M \sin i = 10\text{--}30 M_{\oplus}$  have been discovered by the RV technique (Wright et al. 2010, Exoplanet Orbit Database<sup>10</sup>). Transiting searches for extrasolar planets have detected Neptune-mass planets (Bakos et al. 2010; Hartman et al. 2010) and super-Earths (Léger et al. 2009; Charbonneau et al. 2009). The initial data release from the *Kepler* mission shows substantially increasing planet occurrence with decreasing planet radius (Borucki et al. 2010). Using the large number of low-mass planets, we can statistically study planet properties, occurrence rates, and parameter correlations in ways

previously only possible with higher mass gas-giant planets.

We recently completed an analysis of close-in planet occurrence for 166 G- and K-type dwarf stars in the Eta-Earth Survey (Howard et al. 2010c). We studied the planet detections and non-detections on a star-by-star basis, estimating search completeness. We detected increasing planet occurrence with decreasing planet mass over the mass range 3–1000  $M_{\oplus}$  for planets with orbital periods  $P < 50$  d. We parameterized the planet mass distribution with a power law model from which we extrapolated the occurrence rate of close-in Earth-mass planets, giving  $\eta_{\oplus} = 23_{-10}^{+16}\%$  for planets in the mass range 0.5–2.0  $M_{\oplus}$  with  $P < 50$  d.

Our study also addressed a key prediction of population synthesis models of planet formation (Ida & Lin 2004, 2008; Mordasini et al. 2009)—the expected dearth of close-in, low-mass planets. The “desert” emerges in the simulations from fast migration and accelerating planet growth. Most planets are born near or beyond the ice line and those that grow to a critical mass of several Earth masses either rapidly spiral inward to the host star or undergo runaway gas accretion and become massive gas giants. Our measurements contradict this prediction; we found the highest occurrence rate for planets where theory predicted a dearth, in the regime of 3–30  $M_{\oplus}$  and  $P < 50$  d. Population synthesis models of planet formation are currently unable to explain the distribution of low-mass planets.

To measure the planet occurrence rate as a function of planet mass, our study included previously detected planets, as well as unannounced “planet candidates” (Howard et al. 2010c). Including candidates was necessary to reliably estimate occurrence fractions for low-mass planets, even though the candidates had formal false alarm probabilities (FAPs) as large as 5% at the time of our analysis (June 2010). Such an FAP implies that the planet is very likely to exist, but it’s too high for the secure announcement of a definite planet detection

<sup>1</sup> Based on observations obtained at the W. M. Keck Observatory, which is operated jointly by the University of California and the California Institute of Technology. Keck time has been granted by both NASA and the University of California.

<sup>2</sup> Department of Astronomy, University of California, Berkeley, CA 94720-3411, USA

<sup>3</sup> Space Sciences Laboratory, University of California, Berkeley, CA 94720-7450 USA; howard@astro.berkeley.edu

<sup>4</sup> Department of Astrophysics, California Institute of Technology, MC 249-17, Pasadena, CA 91125, USA

<sup>5</sup> Department of Astronomy, Yale University, New Haven, CT 06511, USA

<sup>6</sup> The Pennsylvania State University, University Park, PA 16802, USA

<sup>7</sup> Center of Excellence in Information Systems, Tennessee State University, 3500 John A. Merritt Blvd., Box 9501, Nashville, TN 37209, USA

<sup>8</sup> Space Telescope Science Institute, 3700 San Martin Dr., Baltimore, MD 21218, USA

<sup>9</sup> Department of Astronomy and Space Physics, Uppsala University, Box 515, 751 20 Uppsala, Sweden

<sup>10</sup> <http://exoplanets.org>

with well-measured orbital parameters. Since then, we continued to intensively observe the planet candidates. Based on the new confirmatory data we report two of them here as bona fide planets. We present HD 97658 b, a close-in, super-Earth planet identified as “Candidate 3” in Howard et al. (2010c), and G1785 b, a Neptune-mass planet identified as “Candidate 7”.

Below we describe the host stars (Section 2) and the RV measurements (Section 3). We analyze these measurements with Keplerian models and assess the probability of spurious detections by computing false alarm probabilities (Sections 4 and 5). We describe photometric observations of HD 97658 and the limits they impose on planetary transits (Section 6). We discuss the radii of these planets and a trend in the host star metallicities among low-mass planets (Section 7).

## 2. STELLAR PROPERTIES

We used Spectroscopy Made Easy (Valenti & Piskunov 1996) to fit high-resolution spectra of HD 97658 (HIP 54906, GJ 3651) and G1785 (HD 192310, HIP 99825), using the wavelength intervals, line data, and methodology of Valenti & Fischer (2005). We further constrained surface gravity using Yonsei-Yale ( $Y^2$ ) stellar structure models (Demarque et al. 2004) and revised *Hipparcos* parallaxes (van Leeuwen 2007), using the iterative method of Valenti et al. (2009). The resulting stellar parameters listed in Table 1 are effective temperature, surface gravity, iron abundance, projected rotational velocity, mass, radius, and luminosity. Both stars are K dwarfs on the main sequence.

HD 97658 lies 0.46 mag below the *Hipparcos* average main sequence ( $M_V$  versus  $B - V$ ) as defined by Wright (2005). This location is consistent with the low metallicity of  $[\text{Fe}/\text{H}] = -0.23 \pm 0.03$ . G1785 is 0.06 mag above the *Hipparcos* average main sequence, consistent with its slightly super-solar metallicity of  $[\text{Fe}/\text{H}] = +0.08 \pm 0.03$ .

Measurements of the cores of the Ca II H & K lines of each spectrum show low levels of chromospheric activity, as quantified by the  $S_{\text{HK}}$  and  $\log R'_{\text{HK}}$ . These chromospheric indices show long-term trends over the six years of measurements, possibly partial activity cycles, so we list ranges of activity indices in Table 1. We detect a weak correlation between individual RVs and  $S_{\text{HK}}$  measurements for HD 97658, but not for G1785. This correlation, with a Pearson linear correlation coefficient of  $r = +0.35$ , does not appear to affect the Keplerian fit of HD 97658 b because the  $S_{\text{HK}}$  time series has negligible Fourier power at or near the adopted orbital period, even when the long-term activity trend is removed.

Following Isaacson & Fischer (2010), and based on  $S_{\text{HK}}$ ,  $M_V$ , and  $B - V$ , we estimate an RV jitter of  $1.5 \text{ m s}^{-1}$  for these stars. This empirical estimate is based on an ensemble of stars with similar characteristics and accounts for RV variability due to rotational modulation of stellar surface features, stellar pulsation, undetected planets, and uncorrected systematic errors in the velocity reduction (Saar et al. 1998; Wright 2005). Jitter is added in quadrature to the RV measurement uncertainties for Keplerian modelling.

## 3. KECK-HIRES VELOCITY MEASUREMENTS

We observed HD 97658 and G1785 with the HIRES echelle spectrometer (Vogt et al. 1994) on the 10-m Keck

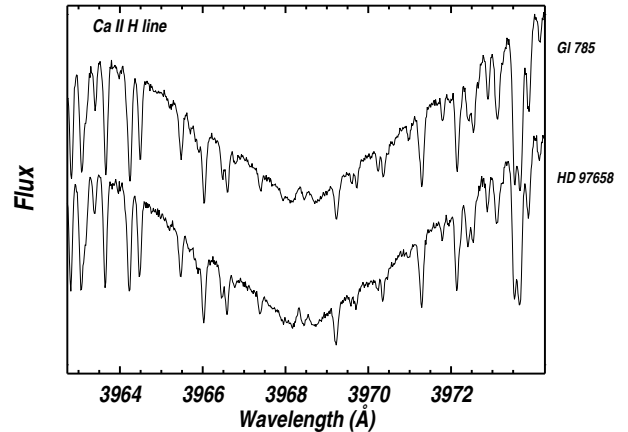


FIG. 1.— Keck-HIRES spectra of the Ca II H line of the early K dwarf stars HD 97658 and G1785. Slight line core emission near 3968 Å indicates modest chromospheric activity.

I telescope. The observations of each star span six years (2004–2010). All observations were made with an iodine cell mounted directly in front of the spectrometer entrance slit. The dense set of molecular absorption lines imprinted on the stellar spectra provide a robust wavelength fiducial against which Doppler shifts are measured, as well as strong constraints on the shape of the spectrometer instrumental profile at the time of each observation (Marcy & Butler 1992; Valenti et al. 1995).

We measured the Doppler shift of each star-times-iodine spectrum using a modelling procedure descended from Butler et al. (1996) as described in Howard et al. (2010b). The velocity and corresponding uncertainty for each observation is based on separate measurements for  $\sim 700$  spectral chunks each  $2 \text{ \AA}$  wide. Once the two planets announced here emerged as candidates (about two years ago) we increased the nightly cadence of measurements and made three consecutive observations per night to reduce the Poisson noise from photon statistics. We calculate one mean velocity for multiple observations in a 2 hr interval.

The highest RV measurement precision using Keck-HIRES has been achieved on chromospherically inactive late G and early K dwarfs, like the two stars presented here. The quietest of these stars are stable over many years at the  $\sim 1.5\text{--}2.0 \text{ m s}^{-1}$  level (Howard et al. 2009, 2010a,b); velocity residuals are due to astrophysical perturbations, instrumental/systematic errors, and Poisson noise. All of the measurements reported here were made after the HIRES CCD upgrade in 2004 August and do not suffer from the higher noise and systematic errors that limited the precision of pre-upgrade measurements to  $\sim 2\text{--}3 \text{ m s}^{-1}$  for most stars.

For each star we constructed a single-planet Keplerian model using the orbit fitting techniques described in Howard et al. (2010a) and the partially linearized, least-squares fitting procedure described in Wright & Howard (2009). The Keplerian parameter uncertainties for each planet were derived using a Monte Carlo method (Marcy et al. 2005) and do not account for correlations between parameter errors. Uncertainties in  $M \sin i$  reflect uncertainties in  $M_*$  and the orbital parameters.

## 4. HD 97658

TABLE 1  
STELLAR PROPERTIES OF HD 97658 AND Gl 785

Parameter	HD 97658	Gl 785
Spectral type	K1 V	K1 V
$M_V$	6.27	6.13
$B - V$	0.80	0.78
$V$	7.78	5.73
$J$	6.203	4.112
$H$	5.821	3.582
$K$	5.734	3.501
Distance (pc)	$21.1 \pm 0.33$	$8.911 \pm 0.024$
$T_{\text{eff}}$ (K)	$5170 \pm 44$	$5144 \pm 50$
$\log g$	$4.63 \pm 0.06$	$4.60 \pm 0.06$
[Fe/H]	$-0.23 \pm 0.03$	$+0.08 \pm 0.03$
$v \sin i$ ( $\text{km s}^{-1}$ )	$0.5 \pm 0.5$	$0.5 \pm 0.5$
$L_*$ ( $L_\odot$ )	$0.34 \pm 0.02$	$0.30 \pm 0.02$
$M_*$ ( $M_\odot$ )	$0.85 \pm 0.02$	$0.78 \pm 0.02$
$R_*$ ( $R_\odot$ )	$0.73 \pm 0.02$	$0.68 \pm 0.02$
$\log R'_{\text{HK}}$	-4.95 to -5.00	-4.90 to -5.02
$S_{\text{HK}}$	0.169 to 0.197	0.169 to 0.226

TABLE 2  
ORBITAL SOLUTION FOR HD 97658 B

Parameter	Value
$P$ (days)	$9.494 \pm 0.005$
$T_c$ (JD - 2,440,000)	$15375.01 \pm 0.64$
$e^a$	$\equiv 0.0$
$K$ ( $\text{m s}^{-1}$ )	$2.75 \pm 0.39$
$M \sin i$ ( $M_\oplus$ )	$8.2 \pm 1.2$
$a$ (AU)	$0.0831 \pm 0.0011$
$N_{\text{obs}}$ (binned)	96
Median binned uncertainty ( $\text{m s}^{-1}$ )	0.74
Assumed jitter ( $\text{m s}^{-1}$ )	1.5
$\sigma$ ( $\text{m s}^{-1}$ )	2.78
$\sqrt{\chi^2_\nu}$	1.59

<sup>a</sup>We adopt a circular orbital solution for this planet.

The RVs and  $S_{\text{HK}}$  values from Keck-HIRES are listed in Table 4. Figure 2 shows a Lomb-Scargle periodogram (Lomb 1976; Scargle 1982) of the RVs with a substantial peak at 9.494 d. We used that period, as well as a wide variety of other trial periods, as seeds for the Keplerian fitting algorithm (Wright & Howard 2009). Our search identified the single-planet orbital solution listed in Table 2 as the best fit.

We also tried fitting the RVs with an eccentric Keplerian model and found a best-fit solution with a nearly identical orbital period and  $e = 0.17 \pm 0.17$ , which is consistent with circular at the  $1\text{-}\sigma$  level. The detection of nonzero eccentricity with better than 95% confidence ( $2\text{-}\sigma$ ) requires approximately  $e/\sigma_e > 2.45$ , where  $\sigma_e = \sigma/K \cdot (2/N)^{0.5}$ ,  $\sigma$  is the measurement uncertainty (including jitter), and  $N$  is the number of uniformly phase-distributed observations (Valenti et al. 2009; Lucy & Sweeney 1971). Our measurements do not meet this criterion. Furthermore, the eccentric model does not improve  $\sqrt{\chi^2_\nu}$  from the circular model. We adopt the circular orbit model in Table 2.

We considered the null hypothesis—that the observed RVs are the chance arrangement of random velocities masquerading as a coherent signal—by calculating two false alarm probabilities (FAPs). Using the method de-

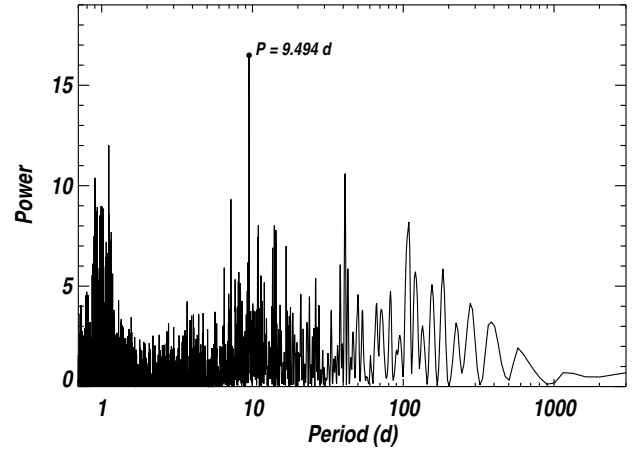


FIG. 2.— Lomb-Scargle periodogram of RV measurements of HD 97658. The tall peak near  $P = 9.494$  d suggests a planet with that orbital period.

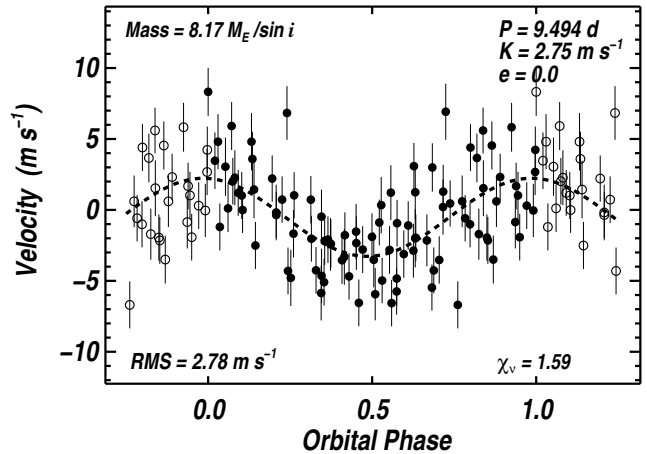


FIG. 3.— Single-planet model for the RVs of HD 97658, as measured by Keck-HIRES. The dashed line shows the best-fit circular orbital solution. Filled circles represent phased measurements while the open circles represent the same velocities wrapped one orbital phase. The error bars show the quadrature sum of measurement uncertainties and  $1.5 \text{ m s}^{-1}$  jitter.

scribed in Howard et al. (2010a), we computed the improvement in  $\Delta\chi^2$  from a constant velocity model to a Keplerian model for  $10^3$  scrambled data sets. In the first FAP test, we allowed for eccentric single-planet orbital solutions in the scrambled data sets. We found that three scrambled data sets had a larger  $\Delta\chi^2$  than the measured velocities, implying an FAP of  $\sim 0.003$  for this scenario. When we restricted the search for orbital solutions to circular orbits, none of the scrambled data sets had a larger  $\Delta\chi^2$  than measured velocities, implying an FAP of less than  $\sim 0.001$ .

The rms of  $2.78 \text{ m s}^{-1}$  about the single-planet model is relatively high compared to our adopted jitter of  $1.5 \text{ m s}^{-1}$  for this chromospherically quiet K dwarf star. This suggests that the measured RVs are compatible with additional detectable planets. We computed a periodogram of the RV residuals to the single-planet fit and found several periods with considerable power in the range  $\sim 40\text{--}200$  d. These peaks correspond to Doppler signals with  $\sim 1.5\text{--}3 \text{ m s}^{-1}$  semiamplitudes. We considered two-planet orbital solutions with  $P_b$  seeded with the

TABLE 3  
ORBITAL SOLUTION FOR GL 785 B

Parameter	Value
$P$ (days)	$74.39 \pm 0.12$
$T_c$ (JD - 2,440,000)	$15173.2 \pm 2.0$
$e$	$0.30 \pm 0.09$
$K$ ( $\text{m s}^{-1}$ )	$4.07 \pm 0.41$
$M \sin i$ ( $M_{\oplus}$ )	$21.6 \pm 2.0$
$a$ (AU)	$0.319 \pm 0.005$
$N_{\text{obs}}$ (binned)	73
Median binned uncertainty ( $\text{m s}^{-1}$ )	0.68
Assumed jitter ( $\text{m s}^{-1}$ )	1.5
$\sigma$ ( $\text{m s}^{-1}$ )	2.06
$\sqrt{\chi^2_{\nu}}$	1.17

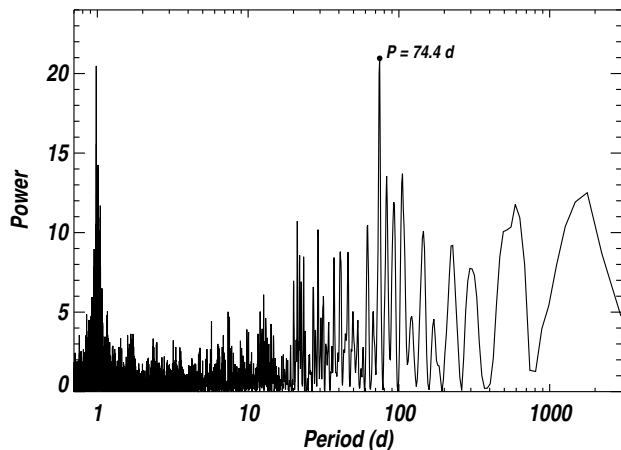


FIG. 4.— Lomb-Scargle periodogram of RV measurements of Gl 785. The tall peak near  $P = 74.4$  d suggests a planet with that orbital period.

best-fit value from the single-planet model and  $P_c$  seeded with peaks in the residual periodogram. We allowed all orbital parameters including eccentricities to float in the two-planet fitting process (Wright & Howard 2009). No two-planet solutions were found with an FAP below 5%. We will continue to observe this star in search of additional planets.

### 5. GL 785

The RVs and  $S_{\text{HK}}$  values from the Keck-HIRES measurements of Gl 785 are listed in Table 5. Figure 4 shows a Lomb-Scargle periodogram (Lomb 1976; Scargle 1982) of the RVs with a substantial peak near 74.4 d. We identify the peaks near 1.0 d as stroboscopic aliases of the sidereal day with the 74.4 d signal and other long periods (Dawson & Fabrycky 2010). We used 74.4 d, as well as a wide variety of other periods, as seed periods for the single-planet Keplerian fitting algorithm (Wright & Howard 2009). Our search identified the single-planet orbital solution listed in Table 2 as the best fit. The orbital eccentricity of  $0.30 \pm 0.09$  is significant at the  $3\text{-}\sigma$  level.

We considered the null hypothesis for the observed periodic signal in the measured RVs of Gl 785 by computing an FAP using the method described in Section 4, including allowing for eccentric solutions with the scrambled data sets. We found that none of the  $10^3$  scrambled data sets had a larger  $\Delta\chi^2$  than the measured velocities, im-

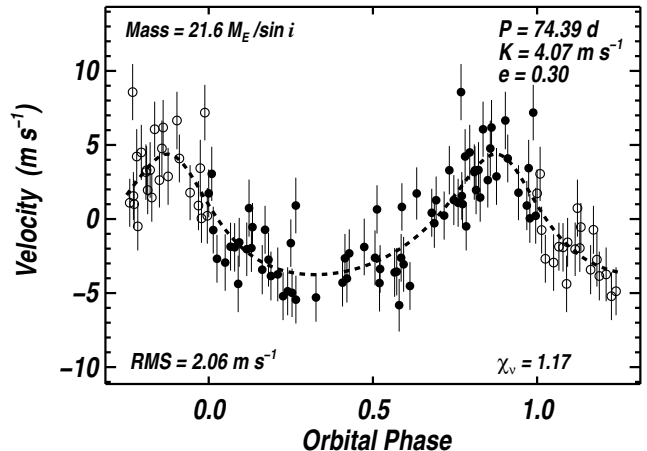


FIG. 5.— Single-planet model for the RVs of Gl 785, as measured by Keck-HIRES. The dashed line shows the best-fit eccentric orbital solution. Symbols have the same meanings as in Figure 3.

plying an FAP of less than  $\sim 0.001$ .

With an rms of  $2.06 \text{ m s}^{-1}$  and a featureless periodogram of velocity residuals to the one-planet model, we do not see evidence for a second detectable planet orbiting Gl 785.

### 6. PHOTOMETRIC OBSERVATIONS

We also acquired photometric observations of HD 97658 with the T12 0.80 m automatic photometric telescope (APT), one of several automatic telescopes operated by Tennessee State University (TSU) at Fairborn Observatory (Eaton et al. 2003). Gl 785 is too far South for this observatory. The APTs can detect short-term, low-amplitude brightness changes in solar-type stars resulting from rotational modulation in the visibility of active regions, such as starspots and plages (e.g., Henry et al. 1995b) and can also detect longer-term variations produced by the growth and decay of individual active regions and the occurrence of stellar magnetic cycles (e.g., Henry et al. 1995a; Hall et al. 2009). The TSU APTs can disprove the hypothesis that RV variations are caused by stellar activity, rather than planetary reflex motion (e.g., Henry et al. 2000a). Several cases of apparent periodic RV variations in solar-type stars induced by the presence of photospheric starspots have been discussed by Queloz et al. (2001) and Paulson et al. (2004). Photometry of planetary candidate host stars is also useful to search for transits of the planetary companions (e.g., Henry et al. 2000b; Sato et al. 2005).

The T12 0.80 m APT is equipped with a two-channel photometer that uses two EMI 9124QB bi-alkali photomultiplier tubes (PMTs) to make simultaneous measurements of a star in the Strömgren  $b$  and  $y$  passbands. The T12 APT is functionally identical to the T8 APT described in Henry (1999). The final data products are differential magnitudes in the standard Strömgren system.

During the three consecutive observing seasons between 2008 January and 2010 June, the APT acquired 318 differential brightness measurements of HD 97658 with respect to the comparison star HD 99518 ( $V = 7.71$ ,  $B - V = 0.343$ , F0). We combined the  $b$  and  $y$  differential magnitudes into  $(b + y)/2$  measurements achieving typi-

cal single measurement precision of 1.5–2.0 mmag (Henry 1999).

The 318 measurements of HD 97658 are plotted in the top panel of Figure 6. The second and third observing seasons have been normalized to match the mean brightness of the first season; the second and third year corrections were 1.75 and 0.70 mmag, respectively. This removes small year-to-year brightness changes in HD 97658 and its comparison star and maximizes sensitivity to brightness variability on night-to-night timescales. The standard deviation of the resulting normalized three-year data set is 1.87 mmag, consistent with measurement error. Periodogram analysis confirms the absence of periodic variability between one and 100 days.

In the second panel of Figure 6, the differential magnitudes are plotted modulo the RV period. Phase 0.0 corresponds to the predicted time of mid-transit (Table 2). A least-squares sine fit gives a semi-amplitude of  $0.09 \pm 0.14$  mmag. This tight limit to photometric variability at the RV period supports the hypothesis that the period RV signal is due stellar reflex motion from a planet in motion.

The observations near phase 0.0 are replotted on an expanded scale in the bottom panel of Figure 6. The solid curve in the two lower panels approximates the depth (0.001 mag) and duration (three hours) of a central transit, derived from the orbital elements and assuming a water/ice composition for the planet. The uncertainty in the time of mid-transit is approximately the width of the bottom panel. The vertical error bar in the lower right of the transit window corresponds to the  $\pm 1.87$  mmag measurement uncertainty of a single observation. The precision and phase coverage of our photometry are insufficient to detect shallow transits.

## 7. DISCUSSION

We announce two low-mass planets that were reported as anonymous “planet candidates” in Howard et al. (2010c). HD 97658 b is a super-Earth planet with minimum mass  $M_P \sin i = 8.2 \pm 1.2 M_\oplus$  in a  $P = 9.494 \pm 0.005$  d orbit around a K1 dwarf star. Gl 785 b is a Neptune-mass planet with minimum mass  $M_P \sin i = 21.6 \pm 2.0 M_\oplus$  in a  $P = 74.39 \pm 0.12$  d orbit also orbiting a K1 dwarf.

We see no evidence for transits of HD 97658 b, although our ephemeris and photometric phase coverage preclude detection of all but the deepest transits of a bloated planet. However, given the *a priori* transit probability of 4%, it is instructive to speculate about the transit signatures of various possible planet compositions. Using the models in Seager et al. (2007), an  $8 M_\oplus$  planet composed of pure Fe,  $\text{MgSiO}_3$ ,  $\text{H}_2\text{O}$ , or H would have radii  $R_{p1} = 1.3, 1.9, 2.4,$  and  $5.5 R_\oplus$ , producing transits of depth 0.3, 0.6, 1.0, and 5.2 mmag, respectively. These homogeneous planet models are oversimplified, but set the scale for admixtures of those ingredients. Transits of planets made of solids and water would have depths of  $\sim 0.3$ –1.0 mmag, while transits of a planet with a significant atmosphere could be much deeper.

We have no constraints on transits of Gl 785 b because the host star is too far South for APT observations. The *a priori* transit probability is 1%. For comparison, we considered the transiting planets HAT-P-11b (Bakos et al. 2010) and HAT-P-26b (Hartman et al. 2010), which have masses  $26 M_\oplus$  and  $19 M_\oplus$  and radii

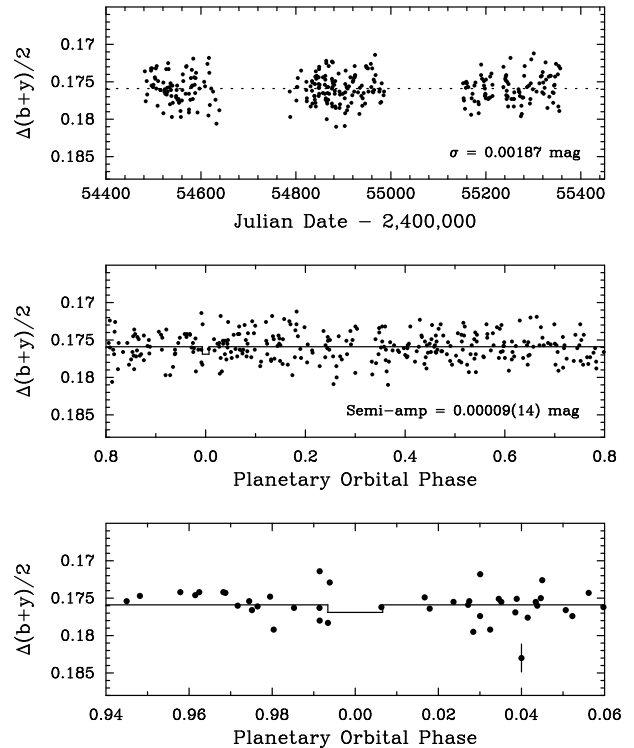


FIG. 6.— Top panel: The 318 Strömgren  $(b + y)/2$  differential magnitudes of HD 97658 plotted against heliocentric Julian Date. The standard deviation of these (normalized) observations from their mean (dotted line) is 1.99 mmag. Middle panel: The observations plotted modulo the RV period. Phase 0.0 corresponds to the predicted time of mid-transit. A least-squares sine fit at the orbital period yields a semi-amplitude of  $0.09 \pm 0.14$  mmag. Bottom panel: The observations near phase 0.0 plotted on an expanded scale. The duration of a central transit is just three hours ( $\pm 0.0066$  phase units); the uncertainty of the transit time is  $\pm 0.64$  days ( $\pm 0.067$  phase units). The precision and phase coverage of our photometry are insufficient to determine whether or not shallow transits occur.

$4.7 R_\oplus$  and  $6.3 R_\oplus$ , respectively. The implied densities, 1.38 and  $0.42 \text{ g cm}^{-3}$ , suggest that these planets have considerable gas fractions. If Gl 785 b has a radius in the range  $4.7$ – $6.3 R_\oplus$ , equatorial transits will be 4.4–7.8 mmag deep. Such transits would be readily detectable from the ground, but would require a considerable observational campaign given the transit time uncertainty of  $\pm 2.0$  d.

Fischer & Valenti (2005) showed that the occurrence of giant planets with  $K > 30 \text{ ms}^{-1}$  correlates strongly with  $[\text{Fe}/\text{H}]$ . This has been interpreted as support for core accretion models of exoplanet formation. However, low metallicity stars might still be able to form less massive planets. Valenti (2010) noted that stars known to host *only* planets less massive than Neptune ( $17 M_\oplus$ ) tend to be metal poor relative to the Sun. HD 97658 ( $[\text{Fe}/\text{H}] = -0.23 \pm 0.03$ ,  $M \sin i = 8.2 \pm 1.2 M_\oplus$ ) and Gl 785 ( $[\text{Fe}/\text{H}] = +0.08 \pm 0.03$ ,  $M \sin i = 21.6 \pm 2.0 M_\oplus$ ) are consistent with this tentative threshold. Before interpreting this physically it is necessary to check for metallicity bias in the subsample of stars around which sub-Neptune mass planets can be detected with current techniques. Further, firmly establishing the apparent anti-correlation between host star metallicity and sub-Neptune mass planet occurrence is best done with a well-controlled sample with uniform detection character-

istics, similar to Fischer & Valenti (2005), or with well-understood detectability, similar to the Eta-Earth Survey.

We thank the many observers who contributed to the measurements reported here. We gratefully acknowledge the efforts and dedication of the Keck Observatory staff, especially Scott Dahm, Hien Tran, and Grant Hill for support of HIRES and Greg Wirth for support of remote observing. We are grateful to the time assignment committees of the University of California, NASA, and NOAO for their generous allocations of observing time. Without their long-term commitment to RV monitoring, these long-period planets would likely remain unknown. We acknowledge R. Paul Butler and S. S. Vogt for many years of contributing to the data presented here. G. W. M. acknowledges NASA grant NNX06AH52G. G. W. H. acknowledges support from NASA, NSF, Tennessee State University, and the State of Tennessee through its Centers of Excellence program. This work made use of the SIMBAD database (operated at CDS, Strasbourg, France), NASA's Astrophysics Data System Bibliographic Services, and the NASA Star and Exoplanet Database (NStED). Finally, the authors wish to extend special thanks to those of Hawai'ian ancestry on whose sacred mountain of Mauna Kea we are privileged to be guests. Without their generous hospitality, the Keck observations presented herein would not have been possible.

TABLE 4  
RADIAL VELOCITIES AND  $S_{\text{HK}}$  VALUES FOR HD 97658

JD - 2440000	Radial Velocity ( $\text{m s}^{-1}$ )	Uncertainty ( $\text{m s}^{-1}$ )	$S_{\text{HK}}$
13398.04143	3.40	0.78	0.197
13748.03543	1.41	0.79	0.190
13806.96152	3.56	0.79	0.187
14085.15873	-2.56	0.83	0.178
14246.87902	-3.08	0.73	0.176
14247.83980	-5.21	1.07	0.175
14248.94470	-0.60	1.16	0.169
14249.80244	1.19	1.24	0.174
14250.83983	-0.72	0.99	0.174
14251.89455	0.64	1.09	0.172
14255.87104	-1.07	0.79	0.174
14277.81740	-1.94	1.04	0.177
14278.83838	1.33	1.03	0.175
14279.83000	1.07	1.00	0.176
14294.76351	-0.07	1.15	0.169
14300.74175	3.77	1.22	0.172
14304.76223	-2.53	1.23	0.174
14305.75910	-0.11	0.81	0.174
14306.77175	3.55	1.15	0.169
14307.74725	4.39	0.83	0.175
14308.75077	6.43	0.84	0.176
14309.74773	5.28	1.23	0.176
14310.74343	4.32	1.20	0.175
14311.74391	7.30	1.15	0.176
14312.74242	-0.26	1.18	0.177
14313.74419	-1.57	1.26	0.178
14314.75074	2.20	1.22	0.174
14455.15432	-5.71	1.18	0.182
14635.79759	-1.70	1.09	0.175
14780.12544	-4.63	1.22	0.177
14807.09051	-2.07	1.26	0.173
14808.15781	2.09	1.30	0.171
14809.14349	2.48	1.16	0.173
14810.02507	8.16	1.29	0.173
14811.11469	2.77	1.28	0.173
14847.11818	-0.50	1.40	0.172

TABLE 4 — *Continued*

JD - 2440000	Radial Velocity ( $\text{m s}^{-1}$ )	Uncertainty ( $\text{m s}^{-1}$ )	$S_{\text{HK}}$
14927.89832	3.45	1.37	0.170
14928.96319	-2.78	1.30	0.170
14929.84171	-3.59	1.22	0.169
14954.97010	1.71	1.13	0.171
14955.92258	2.61	0.59	0.172
14956.90564	3.79	0.64	0.172
14963.96612	4.04	0.66	0.169
14983.87266	0.73	0.70	0.170
14984.90278	-0.75	0.71	0.171
14985.84542	-2.55	0.69	0.171
14986.88960	-3.00	0.69	0.170
14987.89549	-4.46	0.68	0.170
14988.84400	-4.65	0.66	0.170
15041.75244	7.08	1.35	0.169
15164.11579	4.71	1.31	0.173
15188.15802	-0.91	0.76	0.170
15190.13283	-4.78	0.71	0.170
15191.16082	-1.50	0.77	0.170
15192.12820	1.97	0.69	0.171
15193.11592	3.52	0.67	0.172
15197.14316	-0.24	0.71	0.171
15198.06394	-1.62	0.73	0.172
15199.08955	-2.12	0.72	0.172
15256.95777	3.84	0.71	0.180
15285.94217	-1.43	0.68	0.175
15289.83015	0.99	0.64	0.178
15311.78396	-4.52	0.66	0.173
15312.85958	-2.93	0.62	0.173
15313.76751	0.82	0.65	0.172
15314.78094	3.73	0.65	0.172
15317.96407	1.70	0.65	0.174
15318.94543	-3.46	0.67	0.175
15319.90113	-4.34	0.66	0.176
15320.85915	-5.55	0.57	0.180
15321.83386	-2.68	0.62	0.181
15342.87812	-1.40	0.63	0.176
15343.82903	-1.37	0.67	0.176
15344.88076	0.84	0.73	0.175
15350.78135	-4.25	0.62	0.173
15351.88526	-0.04	0.63	0.174
15372.75655	2.37	0.63	0.179
15373.78353	-0.22	0.60	0.179
15374.75786	-0.32	0.61	0.178
15375.77512	-1.73	0.61	0.177
15376.74467	-1.66	0.60	0.177
15377.74062	-0.77	0.59	0.177
15378.74257	3.55	0.65	0.176
15379.79041	0.84	0.63	0.176
15380.74378	6.24	0.60	0.175
15400.74241	1.31	0.72	0.177
15401.76937	2.23	1.41	0.181
15403.73903	-1.12	0.74	0.176
15404.73645	-3.00	0.67	0.181
15405.74110	-3.61	0.69	0.181
15406.73695	-1.93	0.68	0.182
15407.75726	2.44	0.81	0.180
15410.73803	3.93	0.67	0.179
15411.73488	0.95	0.71	0.178
15412.73197	-0.23	1.26	0.178
15413.73512	4.40	0.74	0.163

TABLE 5  
RADIAL VELOCITIES AND  $S_{\text{HK}}$  VALUES FOR GL 785

JD - 2440000	Radial Velocity ( $\text{m s}^{-1}$ )	Uncertainty ( $\text{m s}^{-1}$ )	$S_{\text{HK}}$
13237.92941	1.73	0.59	0.2103
13301.71519	4.76	1.13	0.2260
13549.02705	-2.75	1.02	0.2040
13926.01730	-1.63	0.56	0.2023
13982.83072	-0.75	0.50	0.1963

TABLE 5 — *Continued*

JD - 2440000	Radial Velocity ( $\text{m s}^{-1}$ )	Uncertainty ( $\text{m s}^{-1}$ )	$S_{\text{HK}}$				
14247.08230	-3.60	0.67	0.1955	15106.75946	0.73	1.21	0.1720
14248.11326	-5.82	0.96	0.1950	15109.74590	-3.42	0.71	0.1740
14249.12216	-3.06	1.09	0.1920	15111.71917	-3.85	0.68	0.1753
14252.08848	1.73	0.93	0.1880	15135.74754	0.65	0.64	0.1717
14256.08153	-0.29	0.70	0.1890	15169.68272	0.91	0.72	0.1710
14279.03644	0.22	1.14	0.1920	15290.15433	0.82	0.56	0.1687
14280.04184	3.05	1.05	0.1940	15314.13774	4.09	0.59	0.1710
14286.03340	-4.38	1.18	0.1910	15319.14050	0.05	0.70	0.1667
14294.99649	-3.74	1.02	0.1950	15345.08584	-5.30	0.65	0.1720
14634.06380	8.57	1.15	0.1790	15351.09865	-4.30	0.58	0.1720
14634.98879	4.22	1.08	0.1830	15352.09190	-4.02	0.61	0.1717
14636.03115	4.50	1.10	0.1820	15374.11656	0.23	0.62	0.1743
14637.06862	3.17	1.12	0.1820	15378.11262	1.56	0.59	0.1740
14638.02072	3.31	1.13	0.1830	15379.10643	-0.50	0.62	0.1697
14639.05307	6.06	1.11	0.1850	15381.09845	3.29	0.63	0.1717
14640.12929	2.63	1.08	0.1850	15397.04238	-2.69	0.60	0.1720
14640.97219	6.18	1.10	0.1850	15400.11504	-1.87	0.61	0.1725
14642.09539	2.88	1.20	0.1870	15401.04500	-1.91	0.65	0.1717
14644.10213	6.65	1.23	0.1870	15402.08245	-1.58	0.69	0.1710
14688.96417	-2.62	1.09	0.1820	15404.84477	-1.96	0.58	0.1727
14689.98535	-4.33	1.20	0.1830	15405.08736	-0.55	0.64	0.1710
14723.77286	3.43	1.19	0.1840	15407.93295	-0.73	0.61	0.1753
14724.80700	7.18	1.12	0.1830	15412.01241	-5.21	0.60	0.1730
14808.68992	-2.04	1.01	0.1820	15413.05434	-4.88	0.61	0.1740
14984.07717	-1.89	1.19	0.1750	15414.04948	-4.98	0.65	0.1717
15019.01660	1.78	1.10	0.1740	15414.92114	-5.45	0.58	0.1740
15026.96895	-2.94	1.18	0.1740	15426.03531	-2.65	0.68	0.1717
15042.96436	0.91	1.13	0.1750	15427.00892	-2.32	0.62	0.1710
15073.75665	0.42	0.61	0.1760	15433.99704	-3.37	0.58	0.1737
15074.75183	1.27	0.55	0.1797	15435.78071	-2.41	0.63	...
15077.74110	3.29	0.64	0.1780	15436.75896	-2.30	0.63	...
15078.76189	1.28	0.76	0.1770	15437.76291	-3.55	0.57	0.1747
15079.73545	1.10	0.62	0.1770	15438.76140	-2.62	0.59	0.1770
15080.73918	1.01	0.58	0.1777	15440.75917	-4.52	0.59	0.1773
15084.72917	1.45	0.65	0.1743	15455.73811	1.95	0.63	0.1750

## REFERENCES

- Bakos, G. Á., et al. 2010, *ApJ*, 710, 1724  
 Borucki, W. J., et al. 2010, *ApJ* (submitted), ArXiv:1006.2799  
 Butler, R. P., Marcy, G. W., Williams, E., McCarthy, C., Dossanji, P., & Vogt, S. S. 1996, *PASP*, 108, 500  
 Charbonneau, D., et al. 2009, *Nature*, 462, 891  
 Dawson, R. I., & Fabrycky, D. C. 2010, *ApJ*, 722, 937  
 Demarque, P., Woo, J., Kim, Y., & Yi, S. K. 2004, *ApJS*, 155, 667  
 Eaton, J. A., Henry, G. W., & Fekel, F. C. 2003, in *Astrophysics and Space Science Library*, Vol. 288, *Astrophysics and Space Science Library*, ed. T. D. Oswalt, 189  
 Fischer, D. A., & Valenti, J. 2005, *ApJ*, 622, 1102  
 Fischer, D. A., et al. 2008, *ApJ*, 675, 790  
 Hall, J. C., Henry, G. W., Lockwood, G. W., Skiff, B. A., & Saar, S. H. 2009, *AJ*, 138, 312  
 Hartman, J. D., et al. 2010, *ApJ* (submitted), ArXiv:1010.1008  
 Henry, G. W. 1999, *PASP*, 111, 845  
 Henry, G. W., Baliunas, S. L., Donahue, R. A., Fekel, F. C., & Soon, W. 2000a, *ApJ*, 531, 415  
 Henry, G. W., Eaton, J. A., Hamer, J., & Hall, D. S. 1995a, *ApJS*, 97, 513  
 Henry, G. W., Fekel, F. C., & Hall, D. S. 1995b, *AJ*, 110, 2926  
 Henry, G. W., Marcy, G. W., Butler, R. P., & Vogt, S. S. 2000b, *ApJ*, 529, L41  
 Howard, A. W., et al. 2009, *ApJ*, 696, 75  
 —. 2010a, *ApJ*, 721, 1467  
 —. 2010b, *ApJ* (accepted), ArXiv:1003.3444  
 —. 2010c, *Science*, 330, 653  
 Ida, S., & Lin, D. N. C. 2004, *ApJ*, 604, 388  
 —. 2008, *ApJ*, 685, 584  
 Isaacson, H., & Fischer, D. A. 2010, *ApJ* (accepted), ArXiv:1009.2301  
 Léger, A., et al. 2009, *A&A*, 506, 287  
 Lomb, N. R. 1976, *Ap&SS*, 39, 447  
 Lovis, C., et al. 2006, *Nature*, 441, 305  
 Lucy, L. B., & Sweeney, M. A. 1971, *AJ*, 76, 544  
 Marcy, G. W., & Butler, R. P. 1992, *PASP*, 104, 270  
 Marcy, G. W., Butler, R. P., Vogt, S. S., Fischer, D. A., Henry, G. W., Laughlin, G., Wright, J. T., & Johnson, J. A. 2005, *ApJ*, 619, 570  
 Mayor, M., et al. 2009, *A&A*, 493, 639  
 Mordasini, C., Alibert, Y., & Benz, W. 2009, *Astron. Astrophys.*, 501, 1139  
 Paulson, D. B., Saar, S. H., Cochran, W. D., & Henry, G. W. 2004, *AJ*, 127, 1644  
 Queloz, D., et al. 2001, *A&A*, 379, 279  
 Saar, S. H., Butler, R. P., & Marcy, G. W. 1998, *ApJ*, 498, L153+  
 Sato, B., et al. 2005, *ApJ*, 633, 465  
 Scargle, J. D. 1982, *ApJ*, 263, 835  
 Seager, S., Kuchner, M., Hier-Majumder, C. A., & Militzer, B. 2007, *ApJ*, 669, 1279  
 Valenti, J. A. 2010, in *IAU Symposium*, Vol. 265, *IAU Symposium*, ed. K. Cunha, M. Spite, & B. Barbuy, 403–407  
 Valenti, J. A., Butler, R. P., & Marcy, G. W. 1995, *PASP*, 107, 966  
 Valenti, J. A., & Fischer, D. A. 2005, *ApJS*, 159, 141  
 Valenti, J. A., & Piskunov, N. 1996, *A&AS*, 118, 595  
 Valenti, J. A., et al. 2009, *ApJ*, 702, 989  
 van Leeuwen, F. 2007, *A&A*, 474, 653  
 Vogt, S. S., et al. 1994, in *Proc. SPIE Instrumentation in Astronomy VIII*, David L. Crawford; Eric R. Craine; Eds., Vol. 2198, p. 362  
 Vogt, S. S., et al. 2010, *ApJ*, 708, 1366  
 Wright, J. T. 2005, *PASP*, 117, 657  
 Wright, J. T., & Howard, A. W. 2009, *ApJS*, 182, 205  
 Wright, J. T., et al. 2010, *PASP* (in prep)